Robust differentiation of human enteroendocrine cells from intestinal stem cells

Daniel Zeve[1,2], Eric Stas[1], Xiaolei Yin[3,4,#], Sarah Dubois[1,5], Manasvi S. Shah[1,2], Erin P. Syverson[2,6], Sophie Hafner[1], Jeffrey M. Karp[4,7,8], Diana L. Carlone[1,2,8], David T. Breault[1,2,8,*]

[1]Division of Endocrinology, Boston Children's Hospital, Boston, MA 02115, USA

[2]Department of Pediatrics, Harvard Medical School, Boston, MA 02115, USA

[3]David H. Koch Institute for Integrative Cancer Research, Massachusetts Institute of Technology, Cambridge, MA 02139, USA

[4]Center for Nanomedicine and Division of Engineering in Medicine, Department of Medicine, Brigham and Women's Hospital, Harvard Medical School, Harvard-MIT Division of Health Sciences and Technology, Boston, MA 02115, USA

[5]School of Arts and Sciences, MCPHS University, Boston, MA 02115, USA

[6]Division of Gastroenterology, Boston Children's Hospital, Boston, MA 02115, USA

[7]Broad Institute of MIT and Harvard, Cambridge, MA 02142, USA

[8]Harvard Stem Cell Institute, 7 Divinity Avenue, Cambridge, MA 02138, USA

[*]Corresponding author

[#]Current address: Institute for Regenerative Medicine, Shanghai East Hospital, Frontier Science Center for Stem Cell Research, School of Life Sciences and Technology, Tongji University, Shanghai, China

ABSTRACT

Enteroendocrine (EE) cells are the most abundant hormone-producing cells in humans and are critical regulators of energy homeostasis and gastrointestinal function. Challenges in converting human intestinal stem cells (ISCs) into functional EE cells, *ex vivo*, have limited progress in elucidating their role in disease pathogenesis and in harnessing their therapeutic potential. To address this, we employed small molecule targeting of key transcriptional regulators, GATA4, JNK and FOXO1, known to mediate endodermal development and hormone production, together with directed differentiation of human ISCs. We observed marked induction of EE cell differentiation and gut-derived expression and secretion of SST, 5HT, and GIP upon treatment with various combinations of three small molecules: rimonabant, SP600125 and AS1842856. Robust differentiation strategies capable of driving human EE cell differentiation is a critical step towards understanding these essential cells and the development of cell-based therapeutics.

INTRODUCTION

Enteroendocrine (EE) cells are found throughout the gastrointestinal (GI) tract and represent the most abundant hormone-producing cell type within mammals. EE cells, as a whole, secrete a large variety of hormones, including glucose-dependent insulinotropic polypeptide (GIP), serotonin (5HT), and somatostatin (SST), among others[1,2]. In response to physiological and nutritional cues, EE cells, through the production of these various hormones, are responsible for regulating multiple aspects of gastrointestinal activity and nutritional homeostasis[1,2]. Because of this, EE cells have been implicated in the pathogenesis of gastrointestinal diseases such as irritable bowel syndrome and inflammatory bowel disease, as well as metabolic diseases such as type 2 diabetes[3-5].

Similar to other mature intestinal epithelial cells, EE cells are derived from ISCs, which reside within the crypts of Lieberkuhn[6]. In recent years, much progress has been made understanding the mechanisms underlying ISC self-renewal and differentiation using 3D-enteroid culture[7-10]. Using combinations of growth factors and small molecules targeting specific transcriptional regulators and signaling pathways, intestinal enteroids can either be maintained predominantly as ISCs or differentiated into mature intestinal cells of either the absorptive or secretory lineages[11,12]. For example, maintenance of ISC self-renewal requires activation of canonical Wnt signaling using WNT3a and R-spondin, suppression of bone morphogenic protein (BMP) signaling using Noggin, and inhibition of p38 MAPK signaling using the small molecule SB202190[9-11]. By altering these pathways along with transcriptional regulators, strategies have begun to emerge to direct ISC differentiation into mature intestinal epithelial cell types[8,9,13].

EE cells, as a class, are defined by expression of the neuroendocrine secretory protein Chromogranin A (CHGA), the specific hormone each produces, and location along the GI tract[2,14-16]. Further, multiple transcription factors are critical for EE cell differentiation and function, including neurogenin 3 (NEUROG3), neuronal differentiation 1 (NEUROD1), and pancreatic and duodenal homeobox 1 (PDX1)[1,2,10,17]. The directed differentiation of human EE cells requires the removal of Wnt ligands and inhibition of Notch signaling but, in contrast to mice, human EE cells do not differentiate in the presence of p38 MAPK inhibitors[9,10,16]. While strong mRNA expression of multiple mature EE markers has been observed, limited data exist showing robust protein expression of EE cell markers using small molecule differentiation protocols[8,9,16,18,19].

Additional factors and signaling pathways have also been implicated in EE cell formation and function. For example, GATA Binding Protein 4 (GATA4) plays a role in small intestine formation and plays an important role in specifying EE cell identity, including GIP-expressing cells[20,21]. c-

Jun N-terminal Kinase (JNK) signaling, which has been implicated in regulating ISCs[22], also regulates endocrine cells through its actions on PDX1[23,24]. Inhibition of Forkhead box protein O1 (FOXO1), a transcription factor critical for stem cell function and energy homeostasis[25,26], has been associated with upregulation of multiple endocrine-associated transcription factors and hormones, including NEUROG3 and GIP[27-30]. Finally, BMP4 has been shown to induce the expression of various EE hormones in human intestinal enteroids[16]. However, aside from BMP4, how the above factors impact directed differentiation of EE cells has been largely unstudied.

Here, we establish robust EE cell differentiation protocols for human duodenal enteroids using various combinations of small molecules (rimonabant, SP600125 and AS1842856) designed to alter the activity of GATA4, JNK, and FOXO1, respectively. Treatment with rimonabant and SP600125 leads to marked induction of *CHGA* expression and a corresponding increase in the number of CHGA-positive (CHGA+) cells, as well as in the expression of multiple hormones, including SST, 5HT, and GIP. Separately, treatment with AS1842856 also induced SST, 5HT, and GIP, with an even stronger induction of CHGA+ cells. Comparing levels of hormone secretion, AS1842856 leads to a greater induction of 5HT secretion, but less GIP, whereas rimonabant and SP600125 leads to a greater induction of GIP secretion, but less 5HT. The combination of AS1842856 treatment followed by rimonabant and SP600125 leads to even higher expression of both *SST*, and increased secretion of GIP and 5HT, when compared to rimonabant and SP600125 treatment alone. Together, these robust EE cell differentiation protocols, using small molecules to target GATA4, JNK, and FOXO1, provide important new insights into human EE cell differentiation, with potentially important implications for understanding disease pathogenesis and development of cell-based therapeutics.

RESULTS

Differentiation Media Induces *CHGA* Expression in Human Enteroids

To optimize human EE cell differentiation, we developed a differentiation media (DM, Supplementary Table 1) by combining specific components from published protocols used to induce EE cells[9,12,16,19], including Wnt3a and two additional small molecules associated with endocrine cell differentiation: (1) betacellulin, a ligand of both EGFR and the ErbB4 receptor[31,32] and (2) PF06260933 (PF), a small molecule inhibitor of MAP4K4[33]. Human enteroids were first cultured in growth media (GM, Supplementary Table 1) for two days, allowing for ISC expansion, followed by DM for 12 days (G2D12). Enteroids maintained for 14 days in GM (G14) were used as controls to assess for changes in gene expression. In contrast to previous strategies aimed at generating EE cells over a five day period[9,16], exposure to DM for 12 days was compatible with maintenance of enteroid structural integrity (Fig 1a), possibly due to the continued presence of WNT3a.

To quantify the effectiveness of DM to induce EE cell differentiation, we profiled the gene expression of *CHGA* and other lineage markers, including mucin 2 (*MUC2*, goblet cells), lysozyme (*LYZ*, Paneth cells), intestinal alkaline phosphatase (*ALPI*, enterocytes) and leucine-rich repeat-containing G-protein coupled receptor 5 (*LGR5*, ISCs). In addition, we assessed the expression of transcription factors required for EE differentiation and function (*PDX1, NEUROG3*, and *NEUROD1*), as well as hormones secreted from the duodenum (*SST* and *GIP*). To allow for relative comparison to native tissue expression levels, total RNA from whole mucosal biopsies was included in each qPCR analysis. Exposure of enteroids to G2D12 induced consistent expression of *CHGA, SST*, and *GIP*, with significantly higher levels of *ALPI* and significantly lower expression of *LGR5* when compared to G14 (Fig 1b and Supplementary Fig 1a). Despite G2D12's ability to induce EE and enterocyte markers when compared to G14, their overall expression levels remained considerably lower than whole mucosa. Levels of *PDX1*, *NEUROD1*, *NEUROG3*, *GIP*, and *LYZ* were unchanged compared to G14, with *MUC2* showing a trend towards higher expression in G2D12 enteroids (Fig 1b and Supplementary Fig

1a). Finally, despite induction in *CHGA* mRNA levels in response to G2D12, analysis of CHGA protein using immunofluorescent staining and flow cytometric analysis revealed fewer than 0.1% of all cells to be CHGA+, showing a trend towards higher expression compared with G14 (Fig 1b-1e).

Removal of WNT3a has been shown to aid EE differentiation[9,10,16]. Analysis of enteroids cultured in DM without WNT3a (G2D12-Wnt) revealed undetectable expression levels of *CHGA* and *SST*, reduced *MUC2* expression, and increased *ALPI* expression when compared with enteroids differentiated with WNT3a (G2D12+Wnt) (Fig 1f). To determine whether *CHGA* expression was increased at an earlier time-point during the 14 day differentiation protocol, we performed time-course studies and found that *CHGA* expression was undetectable in enteroids cultured in G2D12-Wnt, while those exposed to G2D12+Wnt showed expression after six days of starting DM (Supplementary Fig 1b). Furthermore, two of the three enteroid lines exposed to G2D12-Wnt showed low total RNA levels around the eighth day of differentiation, consistent with failure to maintain these lines (Supplementary Fig 1c). Therefore, we concluded that the presence of WNT3a in DM is necessary to sustain enteroids in long-term culture (14 days) and is not detrimental to EE differentiation. We also evaluated the impact of including betacellulin and PF in our DM and found that both factors led to increased expression of EE cell markers compared with GM and DM without betacellulin or PF (Supplementary Fig 1d and 1e). Together, these data indicate that our differentiation protocol markedly induced expression of some EE cell marker genes (e.g., *CHGA*), but is not sufficient to induce a significant increase in the number of CHGA+ EE cells compared to undifferentiated controls.

Treatment with Rimonabant and SP600125 Induces EE Lineage Differentiation

To identify additional strategies that might further induce EE cell differentiation, we focused on small molecules shown to target GATA4 and PDX1 activity, key transcriptional regulators

involved in gastrointestinal development and hormone regulation. First, we utilized rimonabant (Rim), a highly selective cannabinoid receptor type I antagonist structurally identical to Compound 7, which was previously shown to increase GATA4 activity *in vitro*[34]. In parallel, we used the small molecule SP600125 (SP) to inhibit JNK, which has been shown to suppress PDX1 activity[23,24].

Separately, both Rim and SP induced expression of multiple EE lineage markers (*CHGA, NEUROD1, NEUROG3, SST*, and *GIP*) when added to DM, with Rim having a much larger effect (Supplementary Fig 2a). Together, the combination of Rim and SP (RSP) yielded even further increases in *SST* and *GIP* expression compared to Rim or SP alone. Both PDX1 and GATA4 expression were unchanged under all experimental conditions (Supplementary Fig 2a). Based on these results, Rim and SP were used in combination for all subsequent experiments. The addition of RSP to DM maintained overall enteroid structural integrity during the 14-day differentiation protocol (Fig 2a and Supplementary Fig 2b). Moreover, compared to enteroids grown in G14 and G2D12, treatment with RSP led to the upregulation of multiple EE markers (*CHGA, PDX1, NEUROD1, NEUROG3, SST*, and *GIP*) to levels approximating whole mucosa (Fig 2b). Other lineage markers were also increased with RSP exposure, including *MUC2*, *ALPI*, and *LGR5* when compared to G14 and G2D12 (Supplementary Fig 2c). Immunofluorescent staining for CHGA showed multiple positive cells within individual enteroids (Fig 2c), with a large majority of enteroids (83%) containing CHGA+ cells (Fig 2d). By comparison, only 1% of enteroids grown in G2D12 were CHGA+ (Fig 2D). Quantitative flow cytometric analysis revealed ~1.3% of all cells treated with RSP were CHGA+, almost seven times the number seen with G2D12 alone (Fig 2e).

Treatment with AS1842856 Induces EE Lineage Differentiation

Next, we assessed the impact of adding AS1842856 (AS), a well-described FOXO1 inhibitor[35], to our differentiation protocol on the differentiation of EE cells. Addition of AS led to the formation of small, spherical enteroids (Fig 3a and Supplementary Fig 3a). Compared to enteroids grown in G14 and G2D12, AS treatment led to the upregulation of multiple EE markers (*CHGA, PDX1, NEUROD1, NEUROG3, and SST*) to levels approximating whole mucosa (Fig 3b). In addition, AS increased expression of other secretory and ISC markers, including *MUC2*, *LYZ*, and *LGR5*, when compared to G14 and G2D12 (Supplementary Fig 3b). Interestingly, the use of AS reduced expression of the enterocyte marker *ALPI,* when compared to G14 and G2D12, suggesting a possible role for FOXO1 inhibition in the induction of the secretory lineage (Supplementary Fig 3b). Immunofluorescent staining revealed CHGA+ cells within a large majority of individual enteroids (85%) (Fig 3c and 3d). By comparison, only 3% of enteroids grown in G2D12 had CHGA+ cells (Fig 3d). Quantitative flow cytometric analysis revealed ~5.6% of all cells exposed to AS to be CHGA+, almost 50 times the number seen with G2D12 alone (Fig 3e).

Treatment with AS1842856 Followed by Rimonabant and SP600215 Increases GIP Expression

Compared to RSP-treated enteroids, AS treatment led to more robust EE differentiation, based on overall induction of multiple EE cell markers and the larger fraction of CHGA+ cells (Fig 2 and 3). Direct comparison of the two protocols revealed that AS exposure led to higher expression of *CHGA, NEUROD1*, *NEUROG3*, and *SST* (Supplementary Fig 4a), consistent with the higher percentage of CHGA+ cells (Fig 2d and 3d). In addition, we noted that RSP induced higher expression of *GIP* compared to AS (Supplementary Fig 4a). Given these results, we next hypothesized that the combination of Rim, AS, and SP (RASP) would further increase expression of both CHGA and GIP. Exposure of enteroids to RASP for the full duration of the

differentiation protocol, however, was not compatible with viable enteroids, as evidenced by their irregular structures and extremely low RNA content (Supplementary Fig 4b and 4c).

We next tested the impact of adding RSP after exposure to AS, reasoning that AS treatment would shunt a larger proportion of cells into the EE lineage, with the later addition of RSP inducing GIP expression in more cells than RSP alone. To identify the appropriate time for the addition of RSP, we performed a time-course analysis of AS-treated enteroids and found that multiple transcription factors required for EE differentiation, including *NEUROD1* and *NEUROG3*, showed increased expression around the fourth day of differentiation. Following this, both *CHGA* and *SST* had detectable transcript levels by the sixth day of differentiation (Supplementary Fig 5a). Given these data, we next hypothesized that AS treatment for six days followed by subsequent exposure to RSP would lead to increased *GIP* expression compared to RSP alone. To test this, we utilized two differentiation strategies: (1) switching from AS to RSP at day six of differentiation (AS→RSP) or (2) adding RSP to AS at day six of differentiation (AS→RASP). Morphologically, AS→RASP produced smaller enteroids compared to other conditions (Supplementary Fig 5b); however, RNA concentrations were consistently above the minimum threshold of 10ng/μL, suggesting improved viability over exposure to RASP for the full duration of the differentiation protocol (Supplementary Fig 5c). Enteroids treated with AS→RASP showed 2-3-fold higher gene expression levels of most EE cell markers when compared to AS (Fig 4a). In contrast, enteroids treated with AS→RSP showed gene expression changes that were either similar or higher than RSP alone but were significantly lower when compared to AS alone, aside from *PDX1* (Fig 4a). Interestingly, although AS→RSP induced expression of *GIP* similar to RSP alone, AS→RASP induced expression levels significantly less than RSP alone (Fig 4a). Furthermore, exposure to AS for the entire differentiation protocol, i.e., AS and AS→RASP, decreased expression of *MUC2* and *ALPI* and increased expression of

LGR5 compared to those that received RSP alone, for any amount of time (Supplementary Fig 5d).

All four differentiation strategies induced a high fraction of CHGA+ enteroids, ranging from 79 to 88% (RSP, 79%; AS, 82%; AS→RSP, 81%; AS→RASP, 88%), as assessed by immunostaining (Fig 4b and 4c). Quantitative flow cytometric analysis revealed ~3.6% of all cells exposed to AS→RSP to be CHGA+, which is between the 1.0% seen in RSP alone and the 6.0% seen in AS alone. AS→RASP had the highest percentage of CHGA+ cells at 7.0%, more than 100 times the number seen with G2D12 alone (Fig 4d). These data reveal that exposure of human enteroids to AS→RASP is the most effective way to induce EE cell differentiation, in terms of mRNA expression of *CHGA*, *NEUROD1*, and *NEUROG3* as well as overall number of CHGA+ cells.

Hormone Production and Secretion Mirror Gene Expression Changes

To assess hormone production and secretion during EE cell differentiation, we next assayed for duodenal-associated hormones in response to the various differentiation conditions. Immunofluorescent staining showed that SST was expressed similarly in all differentiation conditions, aside from G2D12, with 42 to 53% of enteroids containing SST-positive cells (RSP, 45%; AS, 42%; AS→RSP, 53%; AS→RASP, 51%) (Fig 5a and 5b). 5HT was expressed in a higher percentage of enteroids treated with AS throughout the entire differentiation period than those that only received RSP (RSP, 44%; AS, 75%; AS→RSP, 59%; AS→RASP, 76%) (Fig 5c and 5d). Further, an induction in GIP-positive enteroids was detected in response to all differentiation conditions, with the exceptions of G2D12 and AS→RASP (RSP, 66%; AS, 53%; AS→RSP, 56%; AS→RASP, 10%) (Fig 5e and 5f).

Finally, to assess hormone secretion, we assayed conditioned media from each differentiation condition. Exposure to AS alone induced higher levels of 5HT secretion than all other conditions, with AS→RSP conditioned media showing higher levels of 5HT when compared to RSP and AS→RASP (Fig 6a). These patterns persisted when corrected for total DNA content, except that there was only a modest difference between AS→RSP and AS→RASP (Supplementary Fig 6a). Secretion of GIP was highest following exposure to AS→RSP, compared to RSP alone, while AS and AS→RASP treated enteroids revealed no secretion of GIP (Fig 6b and Supplementary Fig 6b). Overall, these data show that RSP and AS, either alone or in combination, can induce protein expression and secretion of multiple duodenal hormones in human enteroids, with specific differences seen between 5HT and GIP depending on RSP and AS exposure.

DISCUSSION

Here, we establish that the addition of the small molecules rimonabant, SP600125 and AS1842856 leads to robust differentiation of human EE cells from duodenal ISCs without the use of transgenic modification. Prior to this, the differentiation of EE cells using only small molecules had mainly been studied in the context of Wnt, Notch, MAPK and BMP signaling, with inhibition of these pathways driving gastrointestinal stem cells into the secretory lineage, and subsequent removal of p38 MAPK inhibition leading to EE cell differentiation[9,16]. Despite these important advances, the overall efficiency of EE differentiation in the majority of these studies is hard to estimate due to their strong reliance on gene expression analysis with little data at the protein level. In this study, we show robust induction of EE differentiation, assessed using gene and protein expression as well as hormone secretion, at levels that approach the native duodenal mucosa.

Many of the studies establishing a role for Wnt, Notch, MAPK, and BMP signaling in EE lineage differentiation have been performed using the enteroid culturing system, which approximates *in vivo* growth and development due to its 3D nature. However, there are significant shortcomings to the analyses of intestinal enteroid differentiation that our study has begun to address. First, RNA expression does not always mirror protein expression, as evidenced by the presence of *GIP* mRNA in AS→RASP enteroids (Fig 4a) with little protein expression noted on immunofluorescence (Fig 5e and 5f) and no secreted protein seen on ELISA (Fig 6b). Further, our study suggests that enteroids grown in G14 are not appropriate as the sole reference in differentiation experiments. For example, G2D12, but not G14, treatment induced expression of *CHGA* mRNA (Fig 1b), but the comparison of enteroid mRNA expression levels to whole duodenal mucosa revealed that G2D12 alone induces only a very low level of *CHGA* compared to native tissue. Moreover, immunodetection of CHGA expression revealed significant heterogeneity between individual enteroids, even when cultured under the same experimental conditions, as evidenced by only a small minority of enteroids and cells staining CHGA+ in G2D12 and the variability in hormone expression using immunofluorescence. These results highlight the limitations of current human EE differentiation protocols.

Multiple EE differentiation protocols using only small molecules have suggested that removal of WNT3a from the base growth medium is critical for secretory lineage differentiation[9,16]. Our results, in contrast, reveal that removal of WNT3a is detrimental to both EE differentiation and long-term viability, as noted by a lack of *CHGA* expression at any time during the differentiation protocol and a marked decrease in total RNA levels with time. This is consistent with a previous study suggesting that maintaining high WNT3a concentrations during differentiation was similar, if not better, at inducing *CHGA* expression than a reduction of WNT3a[19]; however, that study only examined differentiation markers after two days of differentiation. The currently described protocol allows for differentiation over 12 days, much longer than previously published methods

utilizing only small molecules[16,19]. Even though our length of culture and the use of different reagents and source materials could be possible explanations, our data indicate that removal of WNT3a is not necessary for human EE cell differentiation.

We also show that treatment of human enteroids with rimonabant, potentially through activation of GATA4, and in conjunction with a known JNK inhibitor, led to an increase in EE marker expression and EE cell number, compared with G2D12 alone, indicating that GATA4 may play a direct role in human EE differentiation during ongoing epithelial maintenance in the adult intestine. We had similar findings when using a well-described inhibitor of FOXO1, which has been previously implicated in beta cell differentiation[29], but whose role in EE cell differentiation has not been closely examined. It is notable that two recent single cell RNA sequencing studies analyzing human and murine EE lineage differentiation using inducible expression of neurogenin 3 did not identify GATA4, JNK, or FOXO1[15,36], suggesting that they may work upstream of neurogenin 3 or that Rim, SP, and AS are all having off target effects in our enteroid model. For example, while Rim is structurally identical to a described GATA4 activator[34] and induces increased expression of *GIP*, a known target of GATA4[20], it also functions as a dual inhibitor of sterol O-acyltransferase 1 (SOAT1 or ACAT1) and SOAT2 (ACAT2)[37], though these play more of a role in the production of steroid, not peptide, hormones[38].

Our protocol using the small molecules Rim, SP, and AS showed high levels of human EE cell differentiation compared with prior reports[9,16,19]. While transgenic over-expression of *NEUROG3* generated elevated levels of human EE cells[14,36,39], our method avoids the use of genetic techniques while maintaining EE marker expression at levels at or above endogenous levels within the human duodenal mucosa.

Interestingly, exposure of enteroids to combinations of Rim, SP, and AS led to the expression of specific hormones, with Rim and SP inducing GIP expression and AS inducing higher levels of 5HT expression. Exposure to AS→RSP yielded similar levels of GIP mRNA and total GIP+ enteroids, but increased levels of GIP secretion, when compared to RSP alone; however, AS→RASP seemingly inhibited GIP protein production and secretion. AS alone appears to be the most potent inducer of 5HT secretion. Exposure to RSP, with or without AS, induced less 5HT secretion when compared to AS alone. Taken together, these combinatorial data suggest that AS exposure is a potent inducer of 5HT secretion while inhibiting GIP secretion, and exposure to Rim and SP is a potent inducer of GIP secretion while leading to reduced 5HT secretion, when compared to AS-treated enteroids. These data suggest that modulation of GATA4, JNK, and FOXO1, as well as other possible targets, could have multiple effects on EE function, controlling mRNA and protein production, as well as secretion, of multiple hormones.

In summary, addition of Rimonabant, SP600125 and AS1842856 leads to robust differentiation of human EE cells from duodenal ISCs, improving on current methods of differentiation without the use of direct genetic alteration. These studies provide a platform for future studies designed to identify endogenous factors regulating EE differentiation, identifying the role/response of EE cells in human GI disease, and further increasing EE cell numbers to potentially be used as personalized cell therapy.

METHODS

Isolation of human intestinal crypts

Tissues were procured as previously described [40]. In short, de-identified endoscopic biopsies were collected from grossly unaffected tissues in pediatric patients undergoing esophagogastroduodenoscopy at Boston Children's Hospital for gastrointestinal complaints and used for duodenal enteroid derivation. Further, de-identified duodenal resections were collected from adult patients undergoing pancreaticoduodenectomy at Massachusetts General Hospital prior to chemotherapy or radiation therapy for pancreatic carcinoma. Whole mucosal biopsies were generated from the duodenal resections using endoscopic biopsy forceps and used for total RNA isolation. Age and sex of donors can be found in Supplementary Table 2 but were unknown to researchers when experiments were being performed. Only macroscopically normal-appearing tissue was used from patients without a known gastrointestinal diagnosis. Each experiment was performed on at least three independent enteroid lines derived from pediatric biopsy samples. Informed consent and developmentally appropriate assent were obtained at Boston Children's Hospital from the donors' guardian and the donor, respectively. Informed consent was obtained at Massachusetts General Hospital from the donors. All methods were approved and carried out in accordance with the Institutional Review Boards of Boston Children's Hospital (Protocol number IRB-P00000529) and Massachusetts General Hospital (Protocol number IRB-2003P001289).

Resections were briefly washed with pre-warmed DMEM/F12, after which the epithelial layer was separated from the rest of the duodenum manually with sterilized surgical tools then taken for RNA isolation. To isolate crypts, pediatric biopsies were digested in 2mg/mL of Collagenase Type I (Life Technologies, 17018029) reconstituted in Hank's Balanced Salt Solution for 40 minutes at 37°C. Samples were then agitated by pipetting followed by centrifugation at 500 x g for 5 minutes at 4°C. The supernatant was then removed, and crypts resuspended in 200-300µL

of Matrigel (Corning, 356231), with 50µL being plated onto 4-6 wells of a 24-well plate and polymerized at 37°C.

Culturing of human duodenal enteroids *in vitro*

Isolated crypts in Matrigel were grown in growth media (GM) (Supplementary Table 1) and the resulting enteroids were passaged every 6-8 days as needed, with media changes occurring every two days. To passage, Matrigel was mechanically dissociated from the well and resuspended in 500µL of Cell Recovery solution (Corning, 354253) for 40-60 minutes at 4°C. To aid in separating the Matrigel and enteroids, the tubes are gently inverted and then centrifuged at 500 x g for 5 minutes at 4°C. The supernatant was then removed, and enteroids resuspended in Matrigel, followed by mechanical disruption via a bent-tipped pipette. Enteroids were passaged at a 1:2 dilution, with 50µL per well of a 24-well plate. After plating, the enteroids were incubated at 37°C for 10 minutes to allow the Matrigel to set. Once complete, 500µL of GM was added to each well.

For differentiation, enteroids were passaged and grown in GM for two days, to allow for ISC expansion, after which the enteroids were transitioned to differentiation media (DM) with additional small molecules added as described (Supplementary Table 1). Media was changed every two days, with Tubastatin A being removed after the second day of differentiation. Enteroids were taken for analysis after 14 days.

Gene expression analysis

Total RNA was purified from individual wells using TRI®Reagent (Sigma) and the Direct-zol™ RNA kit (Zymo Research), following the manufacturer's protocol. RNA concentration was determined using a NanoDrop™ 1000 spectrophotometer (Life Technologies). RNA was treated

with DNAse (Promega) and reverse transcribed using the High-Capacity cDNA Reverse Transcription Kit (Life Technologies). Gene expression analysis was then performed by Real Time quantitative PCR (qPCR) using a QuantStudio 6 Flex thermocycler (Life Technologies). We used the following Taqman primers from Life Technologies (Supplementary Table 3). *18S* transcripts were used as the internal control and data were expressed using the 2^{-ddCt} method with Ct limit of 40. Fold change, unless otherwise stated, was compared to total RNA derived from adult whole mucosal tissue biopsies.

DNA isolation

To isolate enteroid genomic DNA, 200µL of 50mM NaOH was added to a single well of a 24-well plate and the Matrigel was mechanically dissociated. The samples were then transferred to 1.5mL microcentrifuge tubes and placed in a 95°C heat block for 20 minutes. The tubes were then vortexed, after which 25 µL of 1M Tris-HCl was added. The samples were then centrifuged at 14,000 rpm for 10 minutes. The DNA content of the supernatant was then assayed using a NanoDrop™ 1000 spectrophotometer (Life Technologies).

Immunofluorescence

Immunofluorescence staining was performed as previously described with minor modifications[41]. Enteroids were grown in and isolated from Matrigel as noted above. 1-2 wells from a 24-well plate were washed in 200µL of 1X phosphate-buffered saline (PBS) and moved in suspension to a 1.5mL microcentrifuge tube. Each tube was centrifuged at 800 x g for 5 minutes at 4°C to pellet enteroids. PBS was aspirated, and enteroids were fixed in 200µL of 4% paraformaldehyde (PFA) for 20 minutes on ice, shaking. Each tube was centrifuged again as above, and PFA was aspirated. The enteroids were then resuspended in 500µL of 0.3% Triton-X in PBS and moved to a 48-well plate for the remaining steps. The enteroids were

permeabilized for 30 minutes at room temperature, shaking. Between each step, enteroids were allowed to settle to the bottom of each well, the plate was angled, and the solution aspirated by careful pipetting. Enteroids were then blocked with 5% bovine serum albumin in PBS for 1.5 hours at room temperature, shaking. This was followed by three five-minute washes in 500µL of PBS at room temperature, shaking.

Each well was then incubated in 200µL of primary antibodies diluted in 5% BSA/0.1% Trition-X in PBS at 4°C overnight. Primary antibodies include Chromogranin A (CHGA) (Agilent/Dako, M086901-2, 1:100; Millipore Sigma, HPA017369, 1:100), Serotonin (Abcam, ab66047, 1:100), GIP (Invitrogen, PA5-76867, 1:100) and Somatostatin (R&D Systems, mab2358, 1:100). This was followed by five washes in 500µL of 0.1% Triton-X in PBS for 15 minutes each at room temperature, shaking. 200µL of secondary antibodies, including Alexa Fluor 488- or 647-conjugated anti-mouse (Invitrogen, A-21202, or A-31571, 1:400), Alexa Fluor 488-conjugated anti-rat (Invitrogen, A-21208, 1:400), Alexa Fluor 488-conjugated anti-goat (Invitrogen, A-11055, 1:400) or Alexa Fluor 647-conjugated anti-rabbit (Invitrogen, A-31573, 1:400) diluted in 0.1% Triton-X in PBS were then added to each well and incubated for two hours at room temperature, shaking. Enteroids were then washed as above, then moved to new 1.5mL centrifuge tubes. During the last wash, 4′,6-diamidino-2-phenylindole (DAPI, Life Technologies, D1306) was added at a concentration of 1:1000 for nuclear staining. Enteroids were then centrifuged at 1000 x g for 5 minutes at 4°C to help remove as much PBS as possible. Slides were prepared by drawing three circles with a hydrophobic pen (Vector Laboratories, H-4000). Enteroids were then resuspended in 20µL of Prolong Gold Antifade mountant (Life Technologies, P36930), and droplets placed within hydrophobic circles. The enteroids were spread out to reduce clumping, sealed with a coverslip, and allowed to dry overnight at room temperature. Slides were stored at

4°C for future imaging. Images were acquired using a Nikon upright Eclipse 90i microscope with a 20×/0.75 Plan-Apochromat objective and adjusted for brightness and contrast in Fiji[42].

Quantification of immunofluorescent enteroids

This technique was adapted from a previously described method[43]. Immunofluorescent images were acquired using an Invitrogen EVOS FL 2 Auto microscope (Life Technologies). Representative images of stained enteroids were taken at 2X magnification. The stitched images were then processed in Fiji[42]. The color of the DAPI images was converted to 8-bit grayscale and then the image was smoothed by applying a Gaussian Blur filter (radius = 4, scaled units). Thresholding of the smoothed images was performed using manual adjustment to achieve optimal separation of individual enteroids. Watershed and Find Edges filters were then applied to segment any clumped enteroids. Post-segmentation analysis was performed to outline and count individual enteroids using Analyze Particles (size=4,000-100,000, circularity=0.30-1.00, exclude on edges). Each image was then manually curated to exclude debris and enteroids exhibiting background fluorescence. Any remaining clumped enteroids were manually separated prior to quantification. The outlines generated from the DAPI images were then applied to the corresponding images from the other fluorescent channels. Each color image was converted to 8-bit grayscale and then the HiLo Lookup Table was applied. The threshold gate for stained cells was found by manual adjustment of positively stained enteroids to achieve optimal representation. The threshold gate for each channel was then applied to each experimental condition. The Mean metric was extracted with ROI manager (measure) and compiled for analysis. Enteroids with a Mean value of more than zero were considered positive.

Flow cytometry

Enteroids were incubated in Cell Recovery solution for 40-60 minutes at 4°C to remove the Matrigel and then centrifuged at 500 x g for 5 minutes at 4°C. Enteroids were then incubated in 500µL of TrypLE Express (Life Technologies) at 37°C for 30 minutes and broken up by repeated pipetting using a bent P1000 pipette tip. Each sample was then diluted in 800µL of 20% FBS in Advanced DMEM/F12 and then centrifuged at 500 x g for 5 minutes at 4°C. To mark dead cells, each sample was then incubated in DAPI (1:1000) diluted in 2% FBS/2mM EDTA/calcium-free DMEM for 20 minutes at room temperature, then centrifuged at 500 x g for 5 minutes at 4°C and washed in 2% FBS/2mM EDTA/DMEM. Cells were then incubated in 1% PFA for 15 minutes at room temperature, washed with 2% FBS/PBS and then permeabilized in 0.2% Tween 20 in 2% FBS/PBS for 15 minutes at 37°C. Following centrifugation, cells were resuspended in 0.1% Tween 20/2% FBS/2mM EDTA in PBS with PE-conjugated CHGA (BD Biosciences, 564563, 1:100) or PE-conjugated mouse IgG1, K isotype, (BD Biosciences, 554680, 1:200) or with no antibody (the latter two acting as controls) for 30 minutes on ice. Cells were then washed in 0.1% Tween 20/2% FBS/2mM EDTA in PBS, filtered through a 37-micron mesh, and then analyzed on a BD FACSAria II SORP flow cytometer. For gating strategy, please see Supplementary Figure 7.

ELISA

Hormone quantification for serotonin (Eagle Biosciences/DLD Diagnostika GmbH, SER39-K01) and GIP (MilliporeSigma, EZHGIP-54K) were performed following manufacturer's protocols. For these experiments, enteroids were grown in 48-well plates to aid in concentrating the hormone of interest. Conditioned media was taken on day 14 of differentiation. For GIP quantification, Diprotin A (Tocris, 6019, 100µM), a dipeptidyl peptidase 4 inhibitor, was added daily to the media for the last two days of differentiation to prevent GIP degradation. As a control,

differentiation media not exposed to cells was also evaluated. This value was then subtracted from each experimental sample.

Quantification and statistical analysis

All experiments were repeated using at least three different human enteroid lines and representative data from a single line is shown. For qPCR and flow cytometry studies, each condition was performed using pooled enteroids from 3-5 wells, unless otherwise noted, with each well acting as a single sample. Whole mucosal biopsies from duodenal resections were combined from three different individuals to generate a single reference sample for all experiments.

Prior to statistical analysis, all qPCR data were transformed using $\log_{10}$. When analyzing only two conditions, statistical significance was determined by unpaired, two-tailed Student's t-test, combined with the Holm-Sidak method to control for multiple comparisons. When analyzing more than two conditions, statistical significance was determined by either one-way or two-way ANOVA, followed by Tukey post hoc analysis. Specific conditions were excluded from statistical analysis if the data from 1 or more samples was labeled as not detectable. Statistical details for each experiment can be found within each figure legend.

ACKNOWLEDGEMENTS

We thank members of the Breault laboratory, J. Majzoub, S. Bonner-Weir and J. Turner for helpful discussions. This research was supported by National Institute of Health (NIH) awards T32DK769937, K12DK09472109 and Pediatric Endocrine Society Research Fellowship and Clinical Scholar Awards (to D.Z.), NIH awards HL095722 and UC4DK104165 (to J.M.K.), and support from the Adolph Coors Foundation Award (to D.T.B.).

AUTHOR CONTRIBUTIONS

D.Z. designed and performed experiments, analyzed data, prepared figures and co-wrote the manuscript; E.S. performed experiments, analyzed data and edited the manuscript; X.Y. and E.P.S. performed cell culture experiments; M.S.S. performed flow cytometry experiments; S.D. and S.H. assisted in qPCR and immunofluorescence experiments; J.M.K. provided conceptual advice and reagents; D.L.C. provided conceptual advice and edited the manuscript, and D.T.B. directed the project and co-wrote the manuscript.

COMPETING INTERESTS

The author J.M.K. holds equity in Frequency Therapeutics, a company that has an option to license IP generated by J.M.K and that may benefit financially if the IP is licensed and further validated. The interests of J.M.K. was reviewed and are subject to a management plan overseen by their institutions in accordance with their conflict of interest policies.

Data Availability

This study did not generate any datasets.

Code Availability

This study did not generate or use any previously unreported custom code.

REFERENCES

1 Posovszky, C. Development and Anatomy of the Enteroendocrine System in Humans. *Endocr Dev* **32**, 20-37, doi:10.1159/000475729 (2017).

2 Furness, J. B., Rivera, L. R., Cho, H. J., Bravo, D. M. & Callaghan, B. The gut as a sensory organ. *Nat Rev Gastroenterol Hepatol* **10**, 729-740, doi:10.1038/nrgastro.2013.180 (2013).

3 El-Salhy, M., Hausken, T., Gilja, O. H. & Hatlebakk, J. G. The possible role of gastrointestinal endocrine cells in the pathophysiology of irritable bowel syndrome. *Expert Rev Gastroenterol Hepatol* **11**, 139-148, doi:10.1080/17474124.2017.1269601 (2017).

4 Worthington, J. J., Reimann, F. & Gribble, F. M. Enteroendocrine cells-sensory sentinels of the intestinal environment and orchestrators of mucosal immunity. *Mucosal Immunol* **11**, 3-20, doi:10.1038/mi.2017.73 (2018).

5 Holst, J. J., Vilsboll, T. & Deacon, C. F. The incretin system and its role in type 2 diabetes mellitus. *Mol Cell Endocrinol* **297**, 127-136, doi:10.1016/j.mce.2008.08.012 (2009).

6 Yousefi, M., Li, L. & Lengner, C. J. Hierarchy and Plasticity in the Intestinal Stem Cell Compartment. *Trends Cell Biol* **27**, 753-764, doi:10.1016/j.tcb.2017.06.006 (2017).

7 Yu, H. *et al.* The Contributions of Human Mini-Intestines to the Study of Intestinal Physiology and Pathophysiology. *Annu Rev Physiol* **79**, 291-312, doi:10.1146/annurev-physiol-021115-105211 (2017).

8 Fujii, M. *et al.* Human Intestinal Organoids Maintain Self-Renewal Capacity and Cellular Diversity in Niche-Inspired Culture Condition. *Cell Stem Cell* **23**, 787-793 e786, doi:10.1016/j.stem.2018.11.016 (2018).

9 Sato, T. *et al.* Long-term expansion of epithelial organoids from human colon, adenoma, adenocarcinoma, and Barrett's epithelium. *Gastroenterology* **141**, 1762-1772, doi:10.1053/j.gastro.2011.07.050 (2011).

10 Basak, O. *et al.* Induced Quiescence of Lgr5+ Stem Cells in Intestinal Organoids Enables Differentiation of Hormone-Producing Enteroendocrine Cells. *Cell Stem Cell* **20**, 177-190 e174, doi:10.1016/j.stem.2016.11.001 (2017).

11 Sato, T. & Clevers, H. SnapShot: Growing Organoids from Stem Cells. *Cell* **161**, 1700-1700 e1701, doi:10.1016/j.cell.2015.06.028 (2015).

12 Yin, X. *et al.* Niche-independent high-purity cultures of Lgr5+ intestinal stem cells and their progeny. *Nat Methods* **11**, 106-112, doi:10.1038/nmeth.2737 (2014).

13 Almeqdadi, M., Mana, M. D., Roper, J. & Yilmaz, O. H. Gut organoids: mini-tissues in culture to study intestinal physiology and disease. *Am J Physiol Cell Physiol* **317**, C405-C419, doi:10.1152/ajpcell.00300.2017 (2019).

14 Sinagoga, K. L. *et al.* Deriving functional human enteroendocrine cells from pluripotent stem cells. *Development* **145**, doi:10.1242/dev.165795 (2018).

15 Gehart, H. *et al.* Identification of Enteroendocrine Regulators by Real-Time Single-Cell Differentiation Mapping. *Cell* **176**, 1158-1173 e1116, doi:10.1016/j.cell.2018.12.029 (2019).

16 Beumer, J. *et al.* Enteroendocrine cells switch hormone expression along the crypt-to-villus BMP signalling gradient. *Nat Cell Biol* **20**, 909-916, doi:10.1038/s41556-018-0143-y (2018).

17 Chen, C., Fang, R., Davis, C., Maravelias, C. & Sibley, E. Pdx1 inactivation restricted to the intestinal epithelium in mice alters duodenal gene expression in enterocytes and enteroendocrine cells. *Am J Physiol Gastrointest Liver Physiol* **297**, G1126-1137, doi:10.1152/ajpgi.90586.2008 (2009).

18 Petersen, N. *et al.* Generation of L cells in mouse and human small intestine organoids. *Diabetes* **63**, 410-420, doi:10.2337/db13-0991 (2014).

19 VanDussen, K. L. *et al.* Development of an enhanced human gastrointestinal epithelial culture system to facilitate patient-based assays. *Gut* **64**, 911-920, doi:10.1136/gutjnl-2013-306651 (2015).

20 Jepeal, L. I., Boylan, M. O. & Michael Wolfe, M. GATA-4 upregulates glucose-dependent insulinotropic polypeptide expression in cells of pancreatic and intestinal lineage. *Mol Cell Endocrinol* **287**, 20-29, doi:10.1016/j.mce.2008.01.024 (2008).

21 Walker, E. M., Thompson, C. A. & Battle, M. A. GATA4 and GATA6 regulate intestinal epithelial cytodifferentiation during development. *Dev Biol* **392**, 283-294, doi:10.1016/j.ydbio.2014.05.017 (2014).

22 Biteau, B., Hochmuth, C. E. & Jasper, H. JNK activity in somatic stem cells causes loss of tissue homeostasis in the aging Drosophila gut. *Cell Stem Cell* **3**, 442-455, doi:10.1016/j.stem.2008.07.024 (2008).

23 Kaneto, H. *et al.* Oxidative stress and the JNK pathway in diabetes. *Curr Diabetes Rev* **1**, 65-72 (2005).

24 Tang, C. *et al.* Glucose-Induced beta-Cell Dysfunction In Vivo: Evidence for a Causal Role of C-jun N-terminal Kinase Pathway. *Endocrinology* **159**, 3643-3654, doi:10.1210/en.2018-00566 (2018).

25 Kousteni, S. FoxO1, the transcriptional chief of staff of energy metabolism. *Bone* **50**, 437-443, doi:10.1016/j.bone.2011.06.034 (2012).

26 Tothova, Z. & Gilliland, D. G. FoxO transcription factors and stem cell homeostasis: insights from the hematopoietic system. *Cell Stem Cell* **1**, 140-152, doi:10.1016/j.stem.2007.07.017 (2007).

27 Roy, S. A. *et al.* Dual regulatory role for phosphatase and tensin homolog in specification of intestinal endocrine cell subtypes. *World J Gastroenterol* **18**, 1579-1589, doi:10.3748/wjg.v18.i14.1579 (2012).

28 Garcia-Martinez, J. M., Chocarro-Calvo, A., De la Vieja, A. & Garcia-Jimenez, C. Insulin drives glucose-dependent insulinotropic peptide expression via glucose-dependent regulation of FoxO1 and LEF1/beta-catenin. *Biochim Biophys Acta* **1839**, 1141-1150, doi:10.1016/j.bbagrm.2014.07.020 (2014).

29 Bouchi, R. *et al.* FOXO1 inhibition yields functional insulin-producing cells in human gut organoid cultures. *Nat Commun* **5**, 4242, doi:10.1038/ncomms5242 (2014).

30 Arriola, D. J., Mayo, S. L., Skarra, D. V., Benson, C. A. & Thackray, V. G. FOXO1 transcription factor inhibits luteinizing hormone beta gene expression in pituitary gonadotrope cells. *J Biol Chem* **287**, 33424-33435, doi:10.1074/jbc.M112.362103 (2012).

31 Pagliuca, F. W. *et al.* Generation of functional human pancreatic beta cells in vitro. *Cell* **159**, 428-439, doi:10.1016/j.cell.2014.09.040 (2014).

32 Harskamp, L. R., Gansevoort, R. T., van Goor, H. & Meijer, E. The epidermal growth factor receptor pathway in chronic kidney diseases. *Nat Rev Nephrol* **12**, 496-506, doi:10.1038/nrneph.2016.91 (2016).

33 Zhao, X., Mohan, R., Ozcan, S. & Tang, X. MicroRNA-30d induces insulin transcription factor MafA and insulin production by targeting mitogen-activated protein 4 kinase 4 (MAP4K4) in pancreatic beta-cells. *J Biol Chem* **287**, 31155-31164, doi:10.1074/jbc.M112.362632 (2012).

34 Valimaki, M. J. *et al.* Discovery of Small Molecules Targeting the Synergy of Cardiac Transcription Factors GATA4 and NKX2-5. *J Med Chem* **60**, 7781-7798, doi:10.1021/acs.jmedchem.7b00816 (2017).

35 Yu, F. *et al.* FoxO1 inhibition promotes differentiation of human embryonic stem cells into insulin producing cells. *Exp Cell Res* **362**, 227-234, doi:10.1016/j.yexcr.2017.11.022 (2018).

36 Beumer, J. *et al.* High-Resolution mRNA and Secretome Atlas of Human Enteroendocrine Cells. *Cell*, doi:10.1016/j.cell.2020.04.036 (2020).

37 Netherland, C. & Thewke, D. P. Rimonabant is a dual inhibitor of acyl CoA:cholesterol acyltransferases 1 and 2. *Biochem Biophys Res Commun* **398**, 671-676, doi:10.1016/j.bbrc.2010.06.134 (2010).

38 Ferraz-de-Souza, B. *et al.* Sterol O-acyltransferase 1 (SOAT1, ACAT) is a novel target of steroidogenic factor-1 (SF-1, NR5A1, Ad4BP) in the human adrenal. *J Clin Endocrinol Metab* **96**, E663-668, doi:10.1210/jc.2010-2021 (2011).

39 Chang-Graham, A. L. *et al.* Human Intestinal Enteroids With Inducible Neurogenin-3 Expression as a Novel Model of Gut Hormone Secretion. *Cell Mol Gastroenterol Hepatol* **8**, 209-229, doi:10.1016/j.jcmgh.2019.04.010 (2019).

40 Kasendra, M. *et al.* Development of a primary human Small Intestine-on-a-Chip using biopsy-derived organoids. *Sci Rep* **8**, 2871, doi:10.1038/s41598-018-21201-7 (2018).

41 Dekkers, J. F. *et al.* High-resolution 3D imaging of fixed and cleared organoids. *Nat Protoc* **14**, 1756-1771, doi:10.1038/s41596-019-0160-8 (2019).

42 Schindelin, J. *et al.* Fiji: an open-source platform for biological-image analysis. *Nat Methods* **9**, 676-682, doi:10.1038/nmeth.2019 (2012).

43 Borten, M. A., Bajikar, S. S., Sasaki, N., Clevers, H. & Janes, K. A. Automated brightfield morphometry of 3D organoid populations by OrganoSeg. *Sci Rep* **8**, 5319, doi:10.1038/s41598-017-18815-8 (2018).

Figure 1

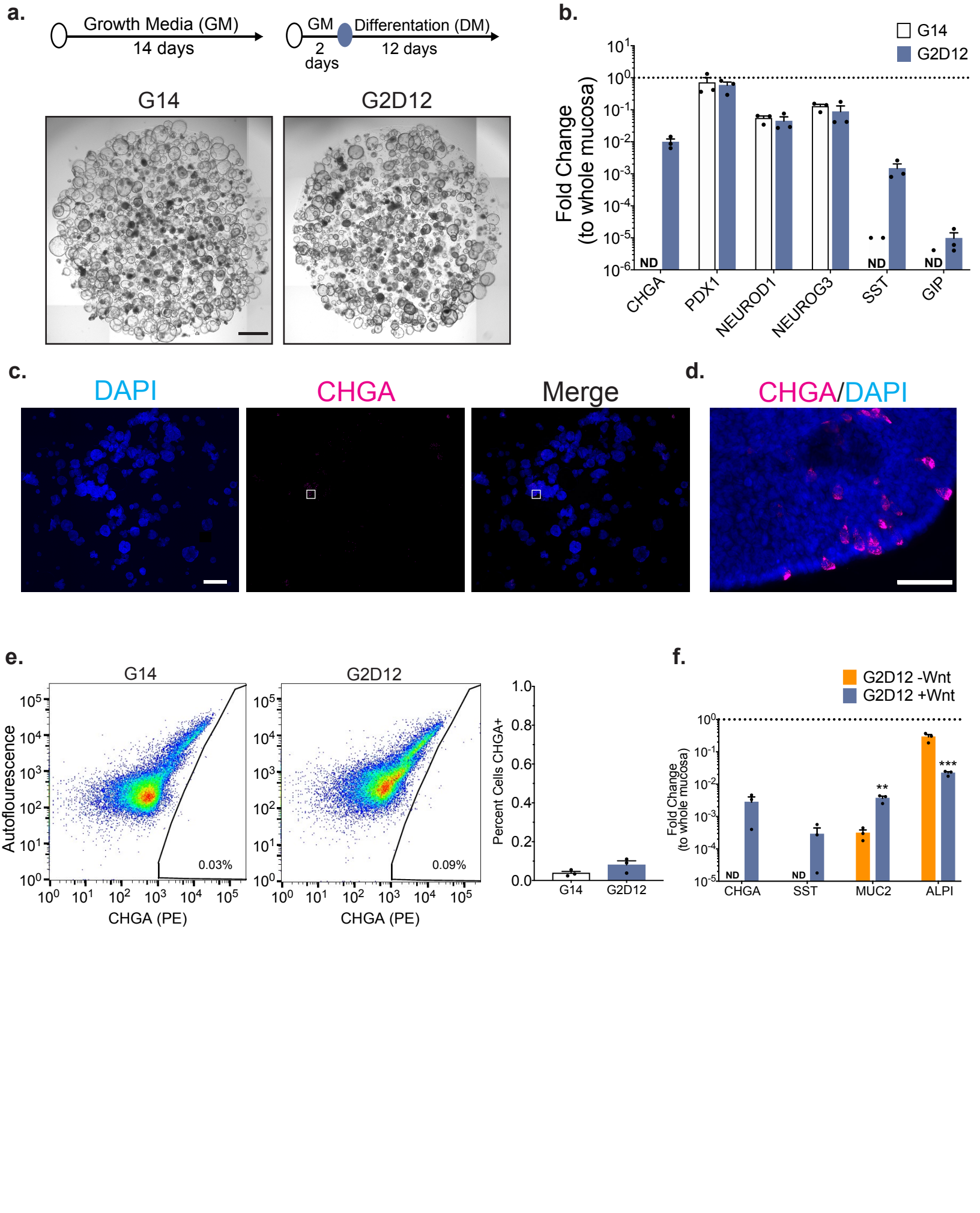

FIGURE LEGENDS

Figure 1. Base Differentiation Media Induces CHGA Expression in a Wnt-dependent Manner

(a) Representative light microscopy of enteroids (whole well) grown in growth media (GM) for 14 days (G14) or two days in GM followed by 12 days in differentiation media (DM, G2D12). Specific culture schematic located above each panel, respectively. Scale bar = 1mm.

(b) qPCR analysis of enteroendocrine (EE) markers of enteroids grown in either G14 or G2D12 compared to whole mucosa and normalized to *18S*. Dotted line denotes expression level in whole mucosa. Representative experiment showing n = 3 wells for each condition from a single enteroid line. CHGA = chromogranin A, PDX1 = pancreatic and duodenal homeobox 1, NEUROD1 = neuronal differentiation 1, NEUROG3 = neurogenin 3, SST = somatostatin, GIP = glucose-dependent insulinotropic peptide, ND = not detectable in 1 or more samples.

(c and d) Representative immunofluorescence staining of CHGA (magenta) in enteroids (whole well) treated with G2D12. Boxed portion in C shown magnified in (D). DNA (4′,6-diamidino-2-phenylindole (DAPI) blue). Scale bars = 1mm (C) and 50μm (D).

(e) Left two panels: Representative flow cytometry plots of CHGA-positive (CHGA+) cells from enteroids grown in either G14 or G2D12. Right panel: Percentage of CHGA+ cells per well. Representative experiment showing n = 3 wells from each condition from single enteroid line.

(f) qPCR analysis of EE gene markers of enteroids grown in either G2D12 without Wnt (G2D12-Wnt) or with Wnt (G2D12+Wnt) compared to whole mucosa and normalized to *18S*. Dotted line denotes expression level in whole mucosa. MUC2 = Mucin 2, ALPI = Intestinal alkaline phosphatase. Representative experiment showing n = 3 wells from each condition from a single enteroid line.

Bars show mean ± SEM, **p < 0.01, ***p < 0.001. Each experiment repeated with at least three different enteroid lines. Specific conditions were excluded from statistical analysis if the data from 1 or more samples was labeled as not detectable.

Figure 2

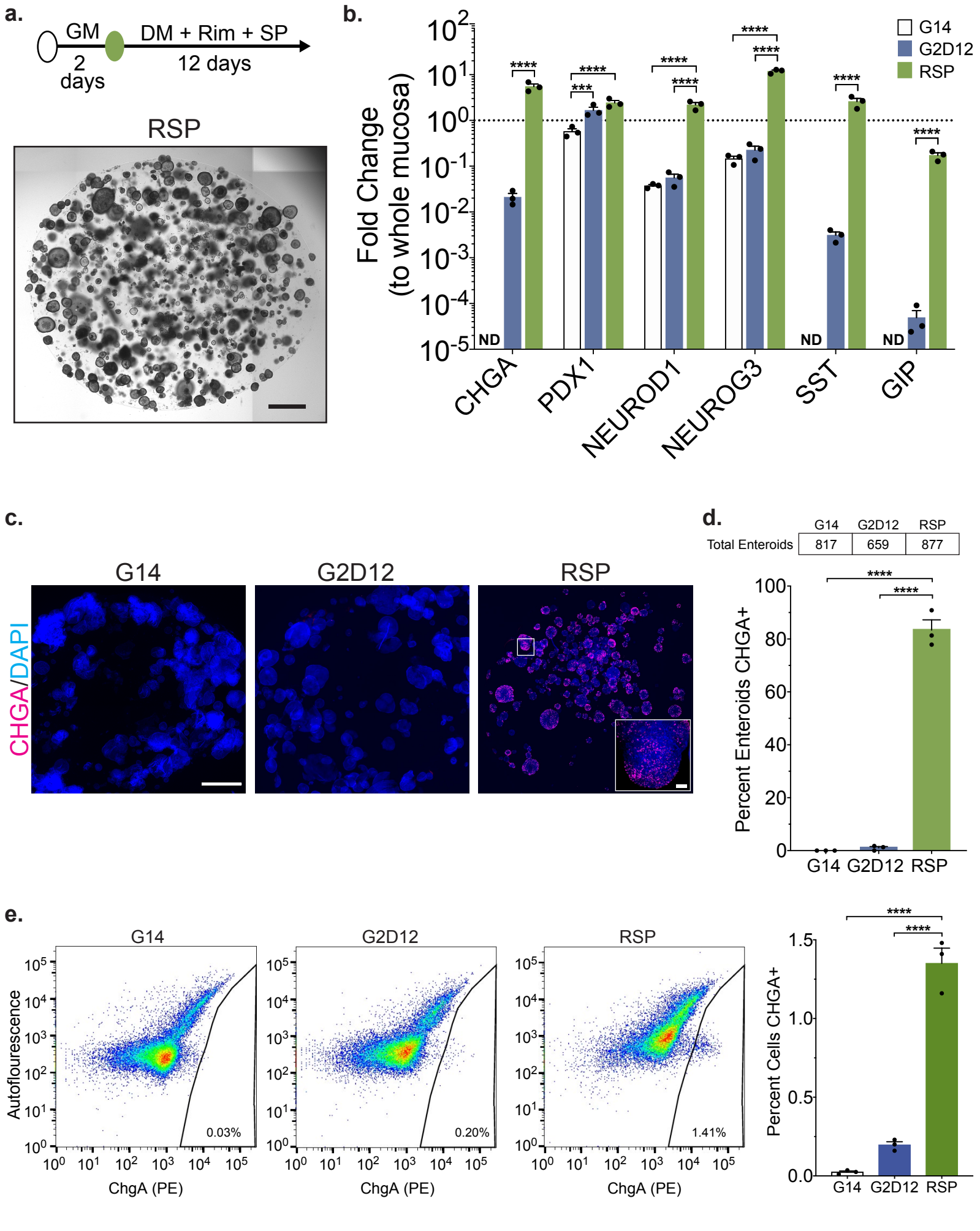

Figure 2. Differentiation with Small Molecules Rimonabant and SP600125 Induces CHGA Expression

(a) Representative light microscopy of enteroids (whole well) grown in G2D12 with rimonabant and SP600125 (RSP). Culture schematic located above panel. Scale bar = 1mm.

(b) qPCR analysis of enteroendocrine markers of enteroids grown in G14, G2D12 or RSP compared to whole mucosa and normalized to *18S*. Dotted line denotes expression level in whole mucosa. Representative experiment showing n = 3 wells from each condition from a single enteroid line. CHGA = chromogranin A, PDX1 = pancreatic and duodenal homeobox 1, NEUROD1 = neuronal differentiation 1, NEUROG3 = neurogenin 3, SST = somatostatin, GIP = glucose-dependent insulinotropic peptide, ND = not detectable.

(c) Representative immunofluorescence staining of CHGA (magenta) in enteroids (whole well) treated with G14, G2D12 and RSP. Boxed portion magnified in lower right corner. Nuclei (4′,6-diamidino-2-phenylindole (DAPI), blue). Scale bars = 1mm and 50μm (boxed portion).

(d) Percentage of enteroids with positive CHGA staining in G14, G2D12 and RSP treatments. Table above graph shows the total number of enteroids examined per condition. Average results are from three separate experiments from three different enteroid lines or passages.

(e) Left three panels: Representative flow cytometry plots of CHGA+ cells from enteroids grown in G14, G2D12 or RSP. Right panel: Quantification of CHGA+ cells per well. Representative experiment showing n = 3 wells from each condition from a single enteroid line.

Bars show mean ± SEM, ***$p < 0.001$, ****$p < 0.0001$. Each experiment repeated with at least three different enteroid lines. Specific conditions were excluded from statistical analysis if the data from 1 or more samples was labeled as not detectable.

Figure 3

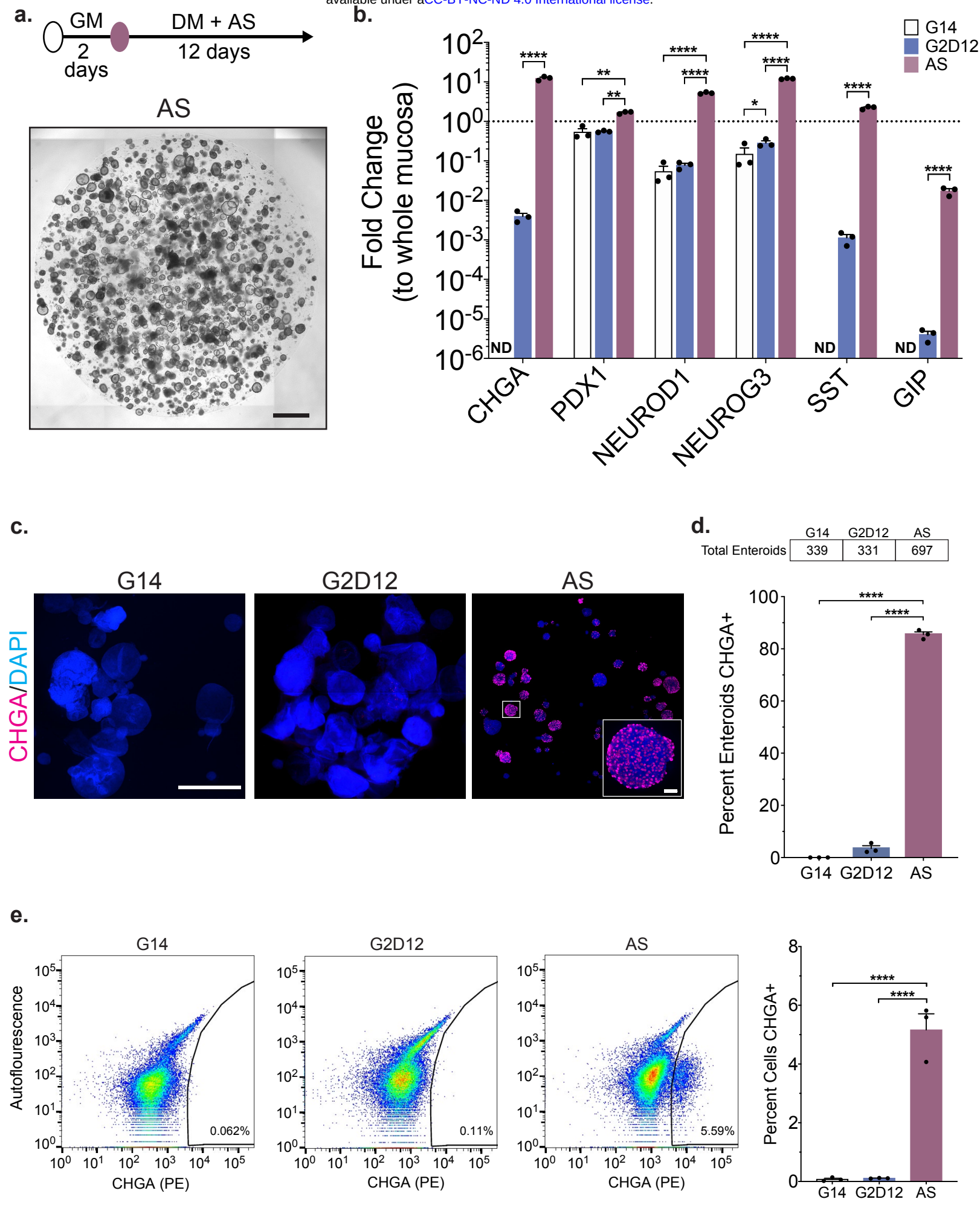

Figure 3. Differentiation with Small Molecule AS1842856 Induces CHGA Expression

(a) Representative light microscopy of enteroids (whole well) grown in G2D12 with AS1842856 (AS). Culture schematic located above panel. Scale bar = 1mm.

(b) qPCR analysis of enteroendocrine markers of enteroids grown in G14, G2D12 or AS compared to whole mucosa and normalized to *18S*. Dotted line denotes expression level in whole mucosa. Representative experiment showing n = 3 wells from each condition from a single enteroid line. CHGA = chromogranin A, PDX1 = pancreatic and duodenal homeobox 1, NEUROD1 = neuronal differentiation 1, NEUROG3 = neurogenin 3, SST = somatostatin, GIP = glucose-dependent insulinotropic peptide, ND = not detectable.

(c) Representative immunofluorescence staining of CHGA (magenta) in enteroids (whole well) treated with G14, G2D12 and AS. Boxed portion magnified in lower right corner. DNA (4′,6-diamidino-2-phenylindole (DAPI), blue). Scale bars = 1mm and 50μm (boxed portion).

(d) Percentage of enteroids with positive CHGA staining in G14, G2D12 and AS treatments. Table above graph shows the total number of enteroids examined per condition. Average results are from three separate experiments from three different enteroid lines or passages.

(e) Left three panels: Representative flow cytometry plots of CHGA+ cells from enteroids grown in G14, G2D12 or AS. Right panel: Quantification of CHGA+ cells per well. Representative experiment showing n = 3 wells from each condition from a single enteroid line.

Bars show mean ± SEM, *$p < 0.05$, **$p < 0.01$, ****$p < 0.0001$. Each experiment repeated with at least three different enteroid lines. Specific conditions were excluded from statistical analysis if the data from 1 or more samples was labeled as not detectable.

Figure 4

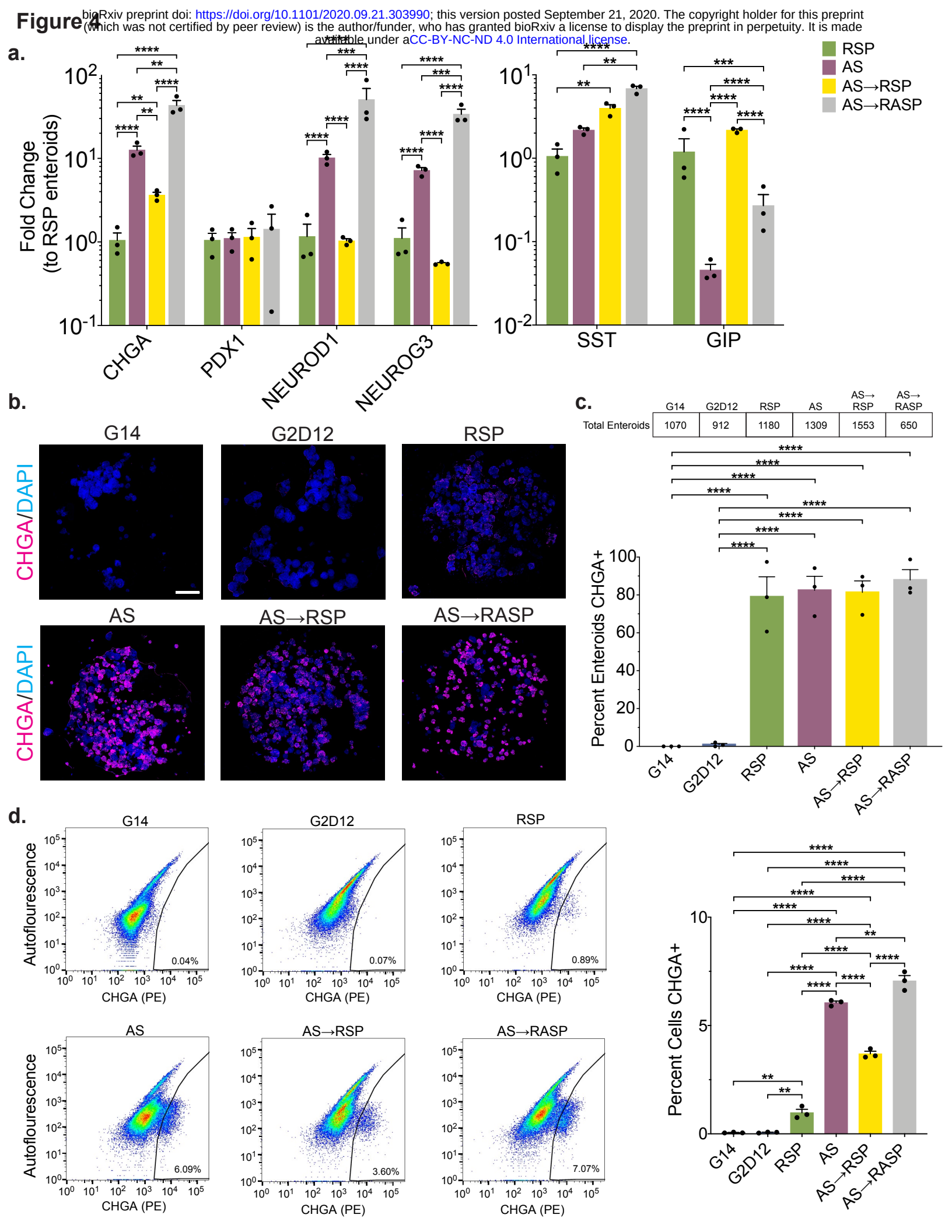

Figure 4. Combinations of AS1842856 and Rimonabant/SP600125 Induce Different Levels of Enteroendocrine Marker Expression

(a) qPCR analysis of enteroendocrine markers of enteroids grown in AS, AS for 6 days, followed by RSP only for 6 days (AS→RSP) and AS for 6 days, followed by AS and RSP for 6 days (AS→RASP) compared to enteroids grown in RSP and normalized to *18S*. Representative experiment showing n = 3 wells from each condition from a single enteroid line. CHGA = chromogranin A, PDX1 = pancreatic and duodenal homeobox 1, NEUROD1 = neuronal differentiation 1, NEUROG3 = neurogenin 3, SST = somatostatin, GIP = glucose-dependent insulinotropic peptide.

(b) Representative immunofluorescence staining of CHGA (magenta) in enteroids (whole well) treated with G14, G2D12, AS, RSP, AS→RSP, and AS→RASP. DNA (4′,6-diamidino-2-phenylindole (DAPI), blue). Scale bar = 1mm.

(c) Percentage of enteroids with positive CHGA staining in G14, G2D12, AS, RSP, AS→RSP, and AS→RASP treatments. Table above graph shows the total number of enteroids examined per condition. Average results are from three separate experiments from three different enteroid lines or passages.

(d) Left six panels: Representative flow cytometry plots of CHGA+ cells from enteroids grown in G14, G2D12, AS, RSP, AS to RSP, and AS to RASP. Right panel: Quantification of CHGA+ cells per well. Representative experiment showing n = 3 wells from each condition from a single enteroid line.

Bars show mean ± SEM, **p < 0.01, ***p < 0.001, ****p < 0.0001. Each experiment repeated with at least three different enteroid lines.

Figure 5

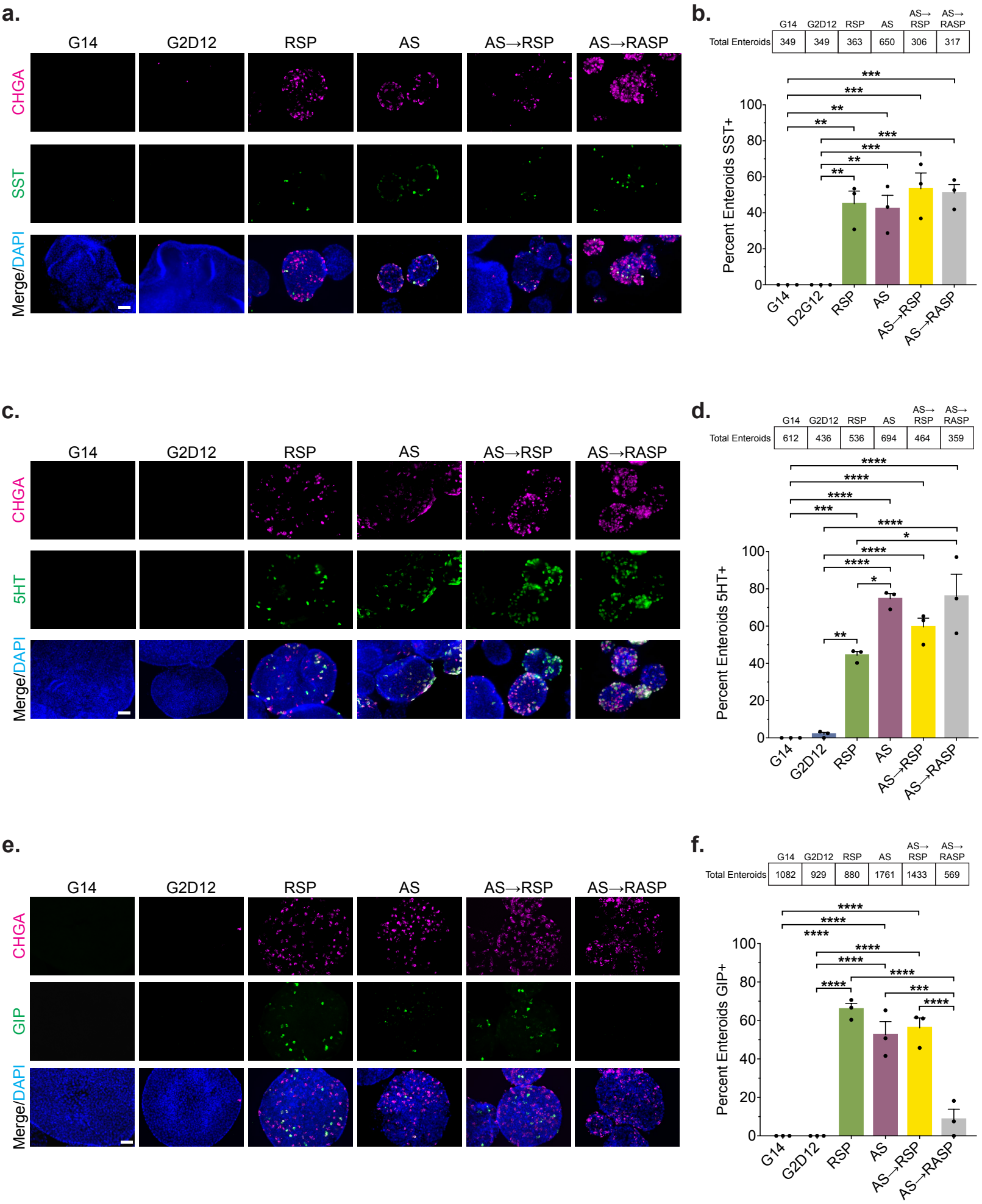

Figure 5. Multiple Differentiation Conditions Induce Hormone Production

(a) Representative immunofluorescence staining of somatostatin (SST, green) and chromogranin A (CHGA, magenta) in enteroids treated with G14, G2D12, AS, RSP, AS→RSP, and AS→RASP. DNA (4′,6-diamidino-2-phenylindole (DAPI), blue). Scale bar = 50μm.

(b) Percentage of enteroids with positive SST staining in G14, G2D12, AS, RSP, AS→RSP, and AS→RASP treatments. Table above graph shows the total number of enteroids examined per condition. Average results are from three separate experiments from three different enteroid lines or passages.

(c) Representative immunofluorescence staining of serotonin (5HT, green) and chromogranin A (CHGA, magenta) in enteroids treated with G14, G2D12, AS, RSP, AS→RSP and AS→RASP. DNA (4′,6-diamidino-2-phenylindole (DAPI), blue). Scale bar = 50μm.

(d) Percentage of enteroids with positive 5HT staining in G14, G2D12, AS, RSP, AS→RSP and AS→RASP treatments. Table above graph shows the total number of enteroids examined per condition. Average results are from three separate experiments from three different enteroid lines or passages.

(e) Representative immunofluorescence staining of glucose-dependent insulinotropic peptide (GIP, green) and chromogranin A (CHGA, magenta) in enteroids treated with G14, G2D12, AS, RSP, AS→RSP, and AS→RASP. DNA (4′,6-diamidino-2-phenylindole (DAPI), blue). Scale bar = 50μm.

(f) Percentage of enteroids with positive GIP staining in G14, G2D12, AS, RSP, AS→RSP, and AS→RASP treatments. Table above graph shows the total number of enteroids examined per condition. Average results are from three separate experiments from three different enteroid lines or passages.

Bars show mean ± SEM, *p < 0.05, **p < 0.01, ***p < 0.001, ****p < 0.0001. Each experiment repeated with at least three different enteroid lines.

Figure 6

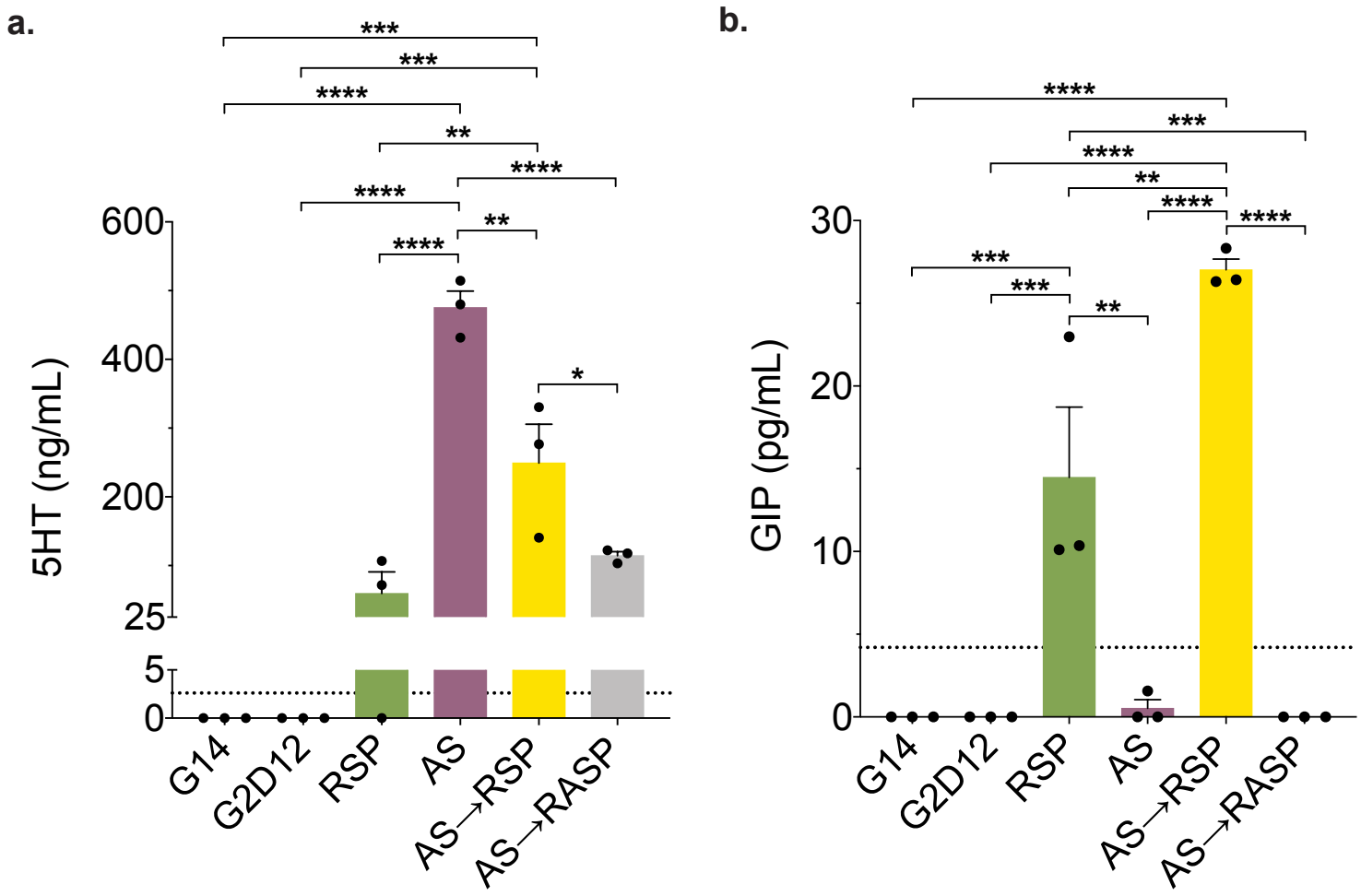

Figure 6. Differentiation Conditions Induce Hormone Secretion

(a) Serotonin (5HT) ELISA of conditioned media from the last two days of differentiation of enteroids grown in G14, G2D12, AS, RSP, AS→RSP, and AS→RASP. Dotted line at 2.6ng/mL represents the lower limit of detection for the assay. Representative experiment showing n = 3 wells from each condition from a single enteroid line.

(b) Glucose-dependent insulinotropic peptide (GIP) ELISA of conditioned media from the last two days of differentiation of enteroids grown in G14, G2D12, AS, RSP, AS→RSP, and AS→RASP. Dotted line at 4.2pg/mL represents the lower limit of detection for the assay. Representative experiment showing n = 3 wells from each condition from a single enteroid line. Bars show mean ± SEM, *p < 0.05, **p < 0.01, ***p < 0.001, ****p < 0.0001. Each experiment repeated with at least three different enteroid lines.